

BDX on-beam background assess and MC validation

M. Battaglieri, A. Celentano, R. De Vita, L. Marsicano
Istituto Nazionale di Fisica Nucleare, Sezione di Genova, 16146 Genova, Italy

M. Bondi, M. De Napoli, N. Randazzo
Istituto Nazionale di Fisica Nucleare, Sezione di Catania, Catania, Italy

G. Kharashvili, E.S. Smith
Jefferson Lab, Newport News, VA 23606, USA

E. Izaguirre
Perimeter Institute for Theoretical Physics, Waterloo, Ontario, Canada, N2L 2Y5

G. Krnjaic
Center for Particle Astrophysics, Fermi National Accelerator Laboratory, Batavia, IL 60510

D. Snowden-Ifft
Occidental College, Los Angeles, California 90041, USA

M. Carpinelli, V. Sipala
Università di Sassari e Istituto Nazionale di Fisica Nucleare, 07100 Sassari, Italy

and The BDX Collaboration

Abstract

In response to the issue raised by JLAB-PAC44 about the experiment proposal *PR-16-001 Dark matter search in a Beam-Dump eXperiment (BDX) at Jefferson Lab* [?] we propose to measure the prompt radiation produced by the interaction of the high intensity 11 GeV electron beam with the Hall-A beam dump. The muon flux will be sampled at different height (with respect-to the beam line), positions and angles downstream of the beam dump to map out the radiation field in the location of the future hall hosting the BDX experiment. In order to realistically assess the beam-on background experienced by the BDX detector, a specimen of the CsI(Tl) crystal from the BDX electromagnetic calorimeter, will be exposed to the radiation min addition to a plastic scintillator hodoscope built specifically for this measurement (BDX-Hodo). The use of a loose trigger will provide further information on beam-related low energy background (dominated by neutrons). Although it will not be possible to directly compare results of this tests with the experimental set up proposed in PR-16-001 that will make use of a different and optimised shielding, the measurement will be extremely useful to validate the MonteCarlo simulation tools (GEANT4 and FLUKA) used to design the new underground facility and optimize the BDX detector.

This report is organised as follow: results of the simulation of the radiation field produced by the interaction of the beam with the dump are reported in Sec. ??; the experimental set-up and the detector is described in Sec. ??; the expected results of the measurement are reported in Sec. ?. Details about cost estimate to run the test, work -and time-planes are reported in the Appendix.

Contents

DRAFT

1 MC simulations

1.1 The Hall-A high-power beam-dump

The Hall A and C use identical high-power absorbing (up to 1 MW) beam-dumps to stop the 11 GeV beam, remnant of beam/target interaction. The dump is made by a set of about 80 aluminum disks, each approximately 40 cm in diameter of increasing thickness (from 1 to 2 cm), for a total length of approximately 200 cm, followed by a solid Al cylinder 50cm in diameter and approximately 100 cm long. They are both cooled by circulating water. The full drawing of the beam-dump is shown in Fig. ???. To increase the radiation shielding, the thickness of the concrete tunnel surrounding the Al dump is about 4-5 m thick.

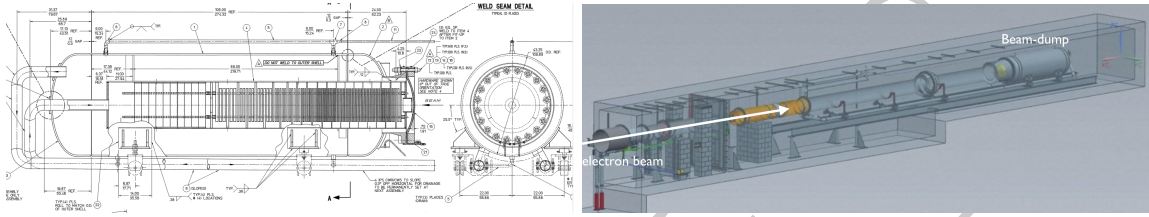


Figure 1: Hall-A beam dump and beam dump enclosure.

1.2 The beam-dump model in FLUKA

The beam-dump geometry and materials have been implemented in FLUKA-2011.2c.5 by the Jefferson Lab Radiation Control Department. Detailed are reported in Ref. [?]. The input card used to run the program includes all physics process and a tuned set of bias to speed up the running time not affecting the results integrity. The μ , n, and γ fluence (differential in angle and energy) per EOT were calculated at XXX cm downstream of the beam window, through a circular area of 105 cm². Figure ?? shows the FLUKA graphic representation and the location of the flux detector. An extension to also include the proper geometry and material composition downstream of the beam-dump has also been implemented. Figure ?? shows the geometry of the concrete bunker surrounding the beam-dump and the soil as implemented in FLUKA.

1.3 The beam-dump model in GEANT4 (GEMC)

The beam-dump model, as well as the geometry and composition of surrounding proximity, has also been implemented in GEANT4 using the GEMC tool [?]. This is a refined version with-respect-to the one used in PR-16-001 [?] that better matches the beam-dump geometry implemented in FLUKA. For a better description of muon transportation, the `G4GammaConversionToMuons` has been added to the standard physics list used in simulations of PR-16-001(`FTFP_BERT_HP + STD + HP`). Particles fluence has been sampled by mean of a flux detector has been positioned in the same location as in the FLUKA model. Figure ?? shows the beam dump and vicinity implemented in GEMC.

1.4 Muons from beam/dump interaction

A comparison of muon fluence downstream of the beam-dump (see above for details about the location) obtained by FLUKA and GEMC are reported in Fig. ???. Considering that low energy muons

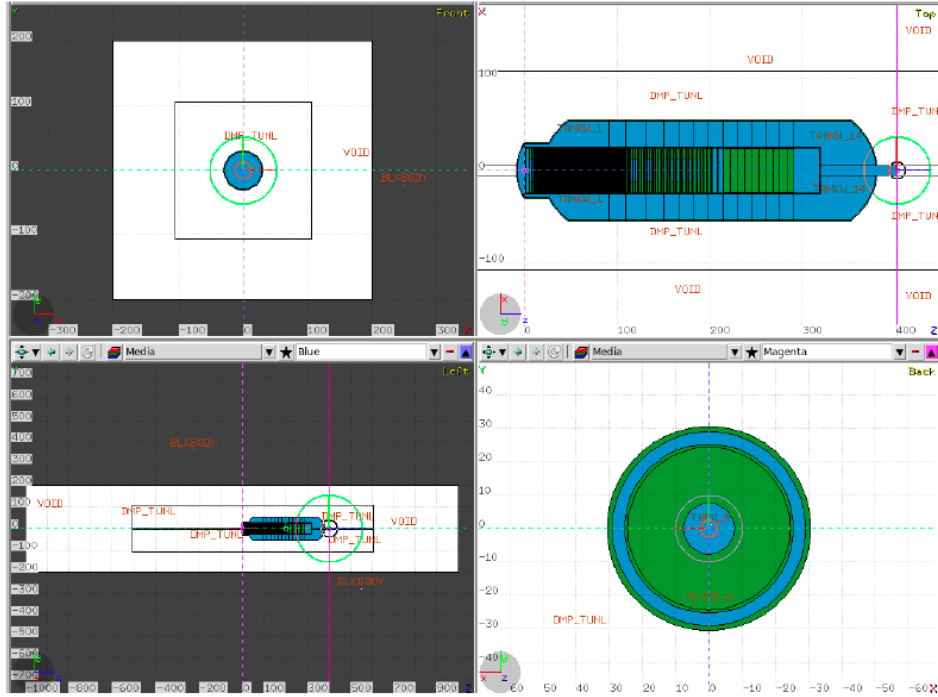


Figure 2: Hall-A beam-dump implementation in FLUKA.

are absorbed by the bunker-head shielding, to keep the GEMC running time reasonable, only particles (all) with energy greater than 100 MeV (`ENERGY_CUT=100*MeV`) has been tracked and sampled. A total of 4×10^9 (9×10^6) EOT have been simulated with GEMC (FLUKA). The comparison of the two simulations shows a perfect agreement in the full energy range where data were generated. In spite of a factor of $\times 100$ less statistics, FLUKA shows, as expected, smaller error bars. This reflects the optimised sizes used by the simulation to generate high statistics for low probability processes keeping the total statistics limited. To penetrate the concrete shielding and the soil, minimum energy of $E_\mu > 4$ GeV is required. With this energy cut, the integrated number of muon per EOT results in $4.8 \pm 0.1 \times 10^{-7}$ ($5.5 \pm 0.2 \times 10^{-7}$) for GEMC and FLUKA respectively. Figure ?? show the correlation between the muon energy and the azimuthal angle (with-respect-to the beam-line): the regions that are populated by both simulations, show again, the same behaviour.

1.5 Sampling and particle transport

The good agreement between two independent simulation tools (FLUKA and GEMC) gives us confidence about reliability of the obtained results. Both methods have pros and cons. FLUKA shows a superior speed in running but a complicated implementation and of selected results (e.g. the final output is given via *scores* such as fluence or distribution in specific location need to be pre-defined). GEMC (GEANT4) tracks particles in all volumes providing a straightforward output (particle four-momenta) in the desired flux detector but requires an un-practical running time to collect a reasonable statistics (in particular when an em shower is involved). In the following we describe how we overtook these difficulties.

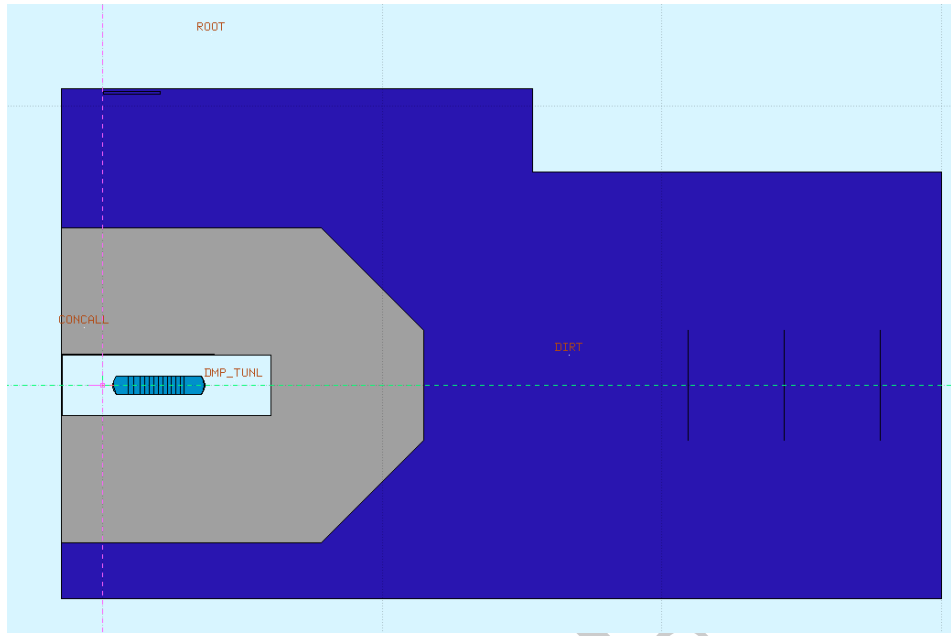


Figure 3: The geometry/composition of the concrete bunker surrounding the beam-dump and the soil as implemented in FLUKA.

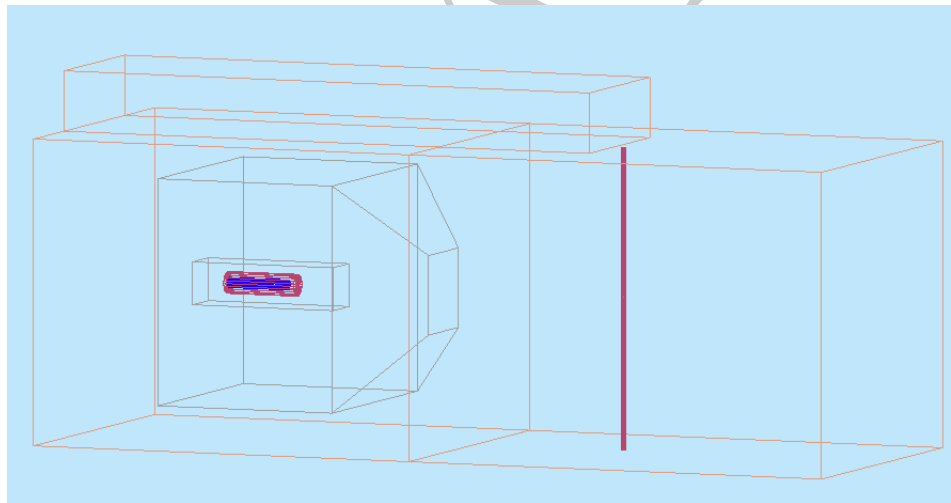


Figure 4: The geometry/composition of the beam-dump, the sourraunding concrete bunker and the soil as implemented in GEMC.

1.5.1 Muons - GEMC

We used GEMC to simulate muons. To make the process more efficient, we followed the procedure described below:

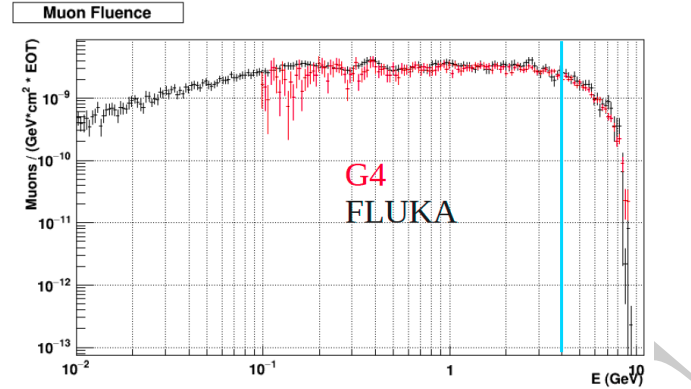


Figure 5: Muon fluence downstream of the beam-dump obtained by FLUKA (black) and GEMC (red). The GEMC simulations started at $E\mu = 100$ MeV.

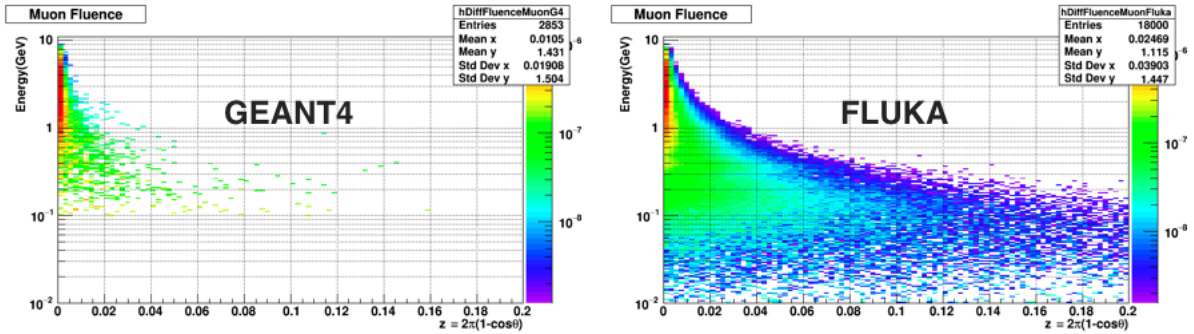


Figure 6: Energy vs. azimuthal angle of muons crossing the flux detector located downstream of the beam-dump obtained by FLUKA and GEMC.

- we used a low statistic sample of EOT to simulate the interaction of the 11 GeV electrons with the beam-dump;
- we sampled the muon flux and variables (momentum, azimuthal angle and transverse position) on a flux detector located downstream of the beam-dump;
- we use the distributions from previous step as input of a custom event-generator to produce a high statistic muon sample;
- we used GEMC to transport muons downstream of the beam dump all the way up the desired location of the BDX-Hodo;
- we implemented the BDX-Hodo response in GEMC to realistically describe the muon detection.

The position where muons are sampled from the primary beam/dump interaction and generated in the custom-made event generator is shown in Fig. ??.

Figure ?? shows the muon distributions (energy vs azimuthal angle and radial distance from the beam line) downstream of the beam-dump, as obtained by the full GEMC simulation of 11

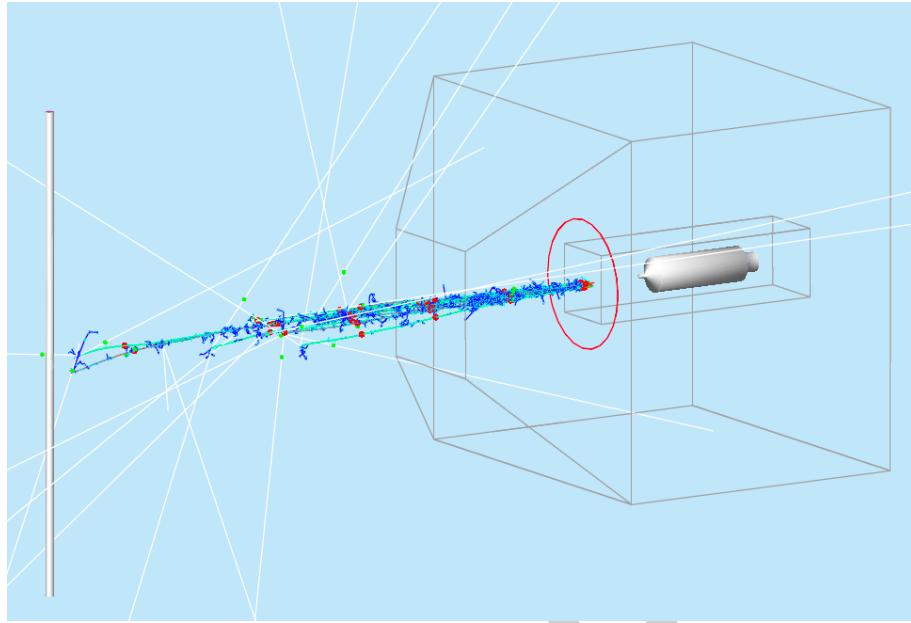


Figure 7: The position of μ sampling/generation.

GeV electrons hitting the beam-dump. The left panel of Fig. ?? shows the comparison one of the two distributions as obtained by the GEMC with the result of the custom event generator. As a check, the right panel of the same figure shows the same comparison in the location of interest, ~ 20 m downstream of the beam-dump. The difference in the error bar size indicates the improvement obtained by this procedure with-respect-to the limited statistic from GEMC.

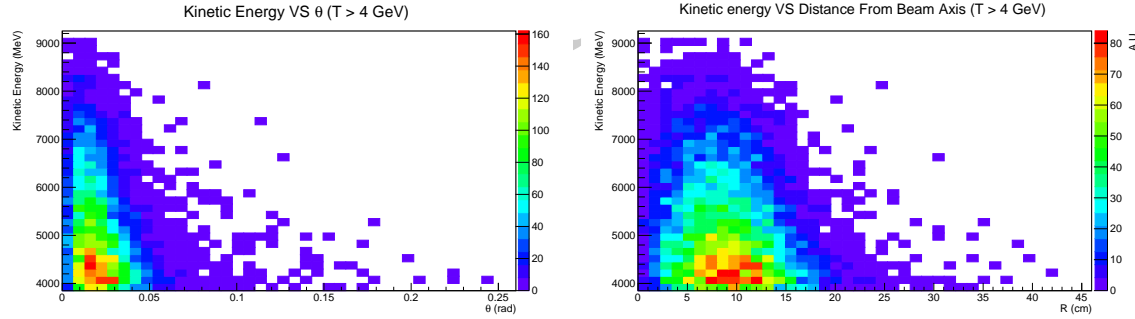


Figure 8: Muon kinetic energy vs. azimuthal angle (left) and distance (right) from the beam-line axes.

1.5.2 Background - FLUKA

We used FLUKA to estimate the background expected in the BDX-Hodo detector. We simulated an 11 GeV electron-beam interacting with the beam-dump and sampled the energy deposition in

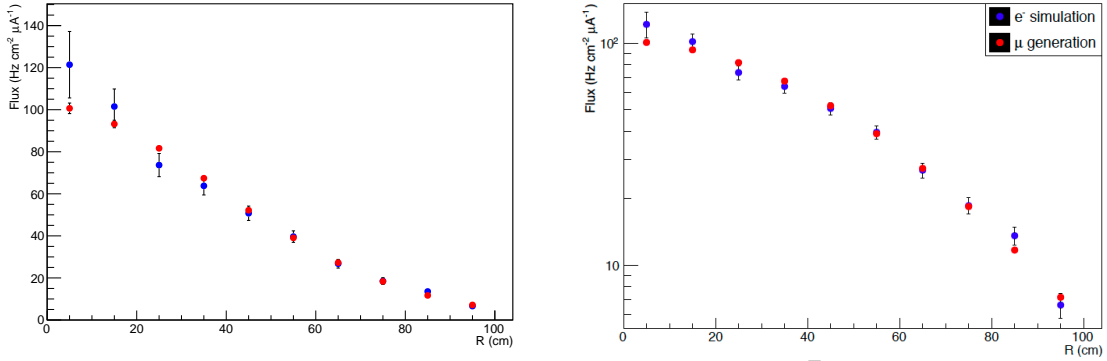


Figure 9: Muon kinetic energy vs. radial distance from the beam-line axes obtained by GEMC (blue) and by the custom event-generator (red) at the sampling/ generation location (left) and in the region of interest (right) ~ 20 m downstream of the beam-dump.

the BDX-Hodo CsI(Tl) crystal when located in the region of interest. Figure ?? shows the energy deposited in the crystal volume. The peak around XX MeV corresponds to MIPs crossing the crystal. The flux of MIPs derived integrating the peak over a smooth background is in good agreement with the number of muons obtained by the full muon simulation with GEMC. The remaining hits are mainly due to high energy neutrons interacting with the crystals and low energy neutrons captured by surrounding material. More details are reported in Sec. ???. It's interesting to note that the spectrum of high energy neutrons , $T_{n,i} > 100$ MeV, (sampled downstream of the dump) obtained by GEMC is in good agreement with FLUKA (see Fig. ??). The agreement indicates that, in this energy range, both simulation tools are reliable.

Another interesting aspect of the neutron spectrum is shown in Fig. ???. Here the energy spectrum (sampled downstream of the dump) obtained by FLUKA by RadCon (Ref. [?]) is compared to the same plot obtained in our FLUKA simulations. The difference of the two runs is only in the different implementation of beam-dump vault: a detailed description of the material surrounding the dump, that includes air and concrete, versus a simplified geometry/material description. The effect is clearly visible in the low energy part of the spectrum (while the high energy part is almost identical) proving that a detailed description of the dump enclosure is necessary to correctly describe the produced backgrounds.

Muon and background flux at the location of interest will be discussed in details in the Sec. ?? after presenting in the next Section, the proposed experimental set up and the BDX-Hodo detector.



Figure 10: Energy deposited in the BDX-Hodo CsI(Tl) crystal by ALL crossing particles. The crystal has been located in the region of interest ~ 20 m downstream of the beam-dump.

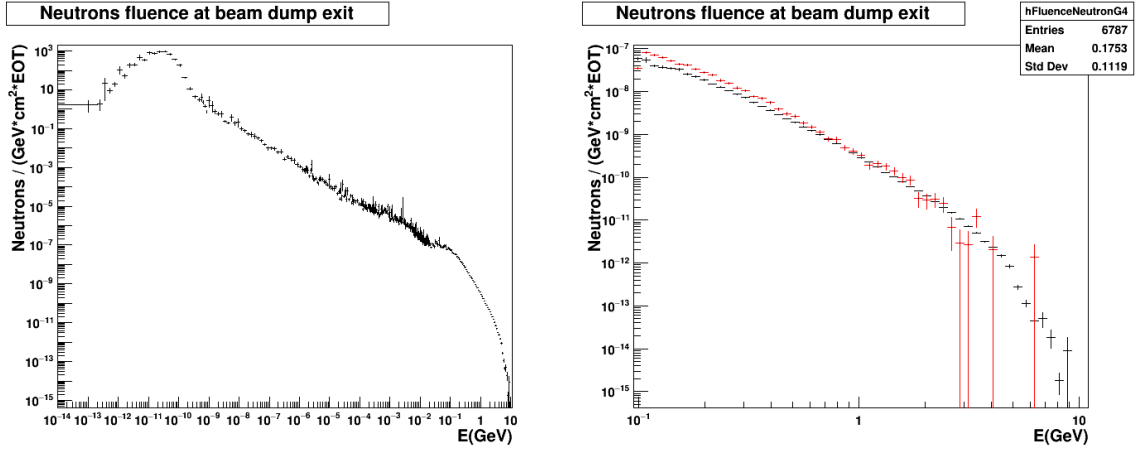


Figure 11: Neutron spectrum downstream of the the dump obtained by full FLUKA simulation (left). The right panel shows the comparison between FLUKA (black) and GEMC (red) for the high energy part pf the spectrum.

Figure 12: Neutron differential fluence downstream of HPBD

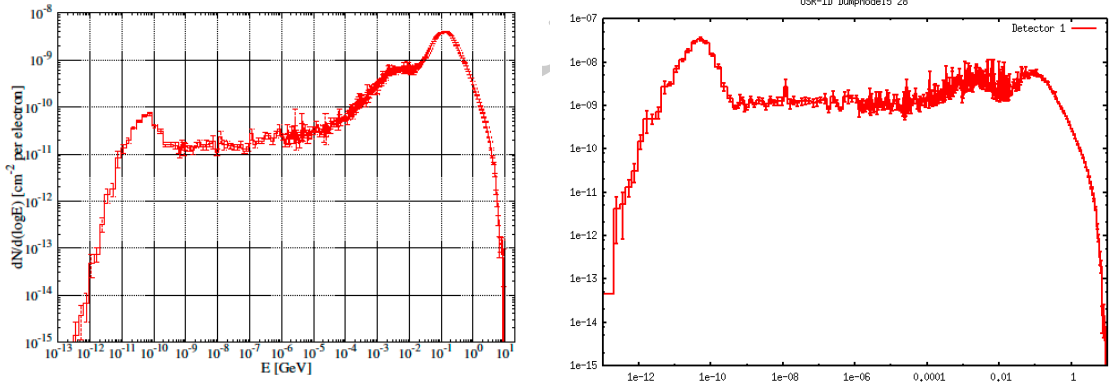


Figure 12: Comparison of neutron energy spectrum obtained by FLUKA, sampled downstream of the beam-dump with a simplified geometry (left) and including vault sourounding materials (right). The numeber of low energy neutrons significantly increases when the reflection on the wall is considered.

2 Test set-up



Hall A Beam Dump / C1

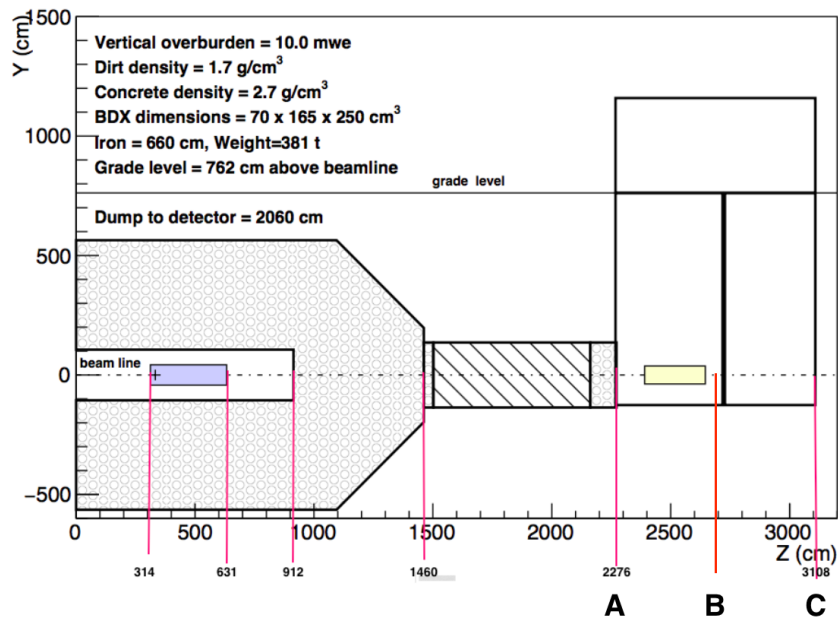


Figure 13: The area downstream of the Hall-A beam-dump and the studied test locations.

2.1 Detector location

The area downstream of Hall-A beam-dump is shown in Fig. ?? together with the corresponding location with-respect-to the new underground facility proposed in PR-16-001 [?]. The three posi-

tions, indicated with markers **A**, **B** and **C**, correspond to the hall entrance (22.4 m downstream of the beam-dump entrance), a point in the middle (25.2 m) and the exit (28 m), respectively. The experimental set-up we are proposing assumes to dig a well and insert a pipe in one (or more) of these locations. The BDX-Hodo detector will be lowered in the pipe and muon flux sampled at different height wrt. the beam-line nominal height. The muon flux profiles in Y (vertical direction), measured in different location in Z (distance from the dump) will allow us to compare the absolute and relative MC predictions.

2.2 The BDX-Hodo detector

The detector used to measure the muon and neutron radiation in the proximity of the new BDX underground facility will make use of a BDX ECal CsI(Tl) crystal sandwiched between a set of segmented plastic scintillators. A CAD representation as well as cuts with sizes are shown in Fig. ???. The front of the crystal will be equipped with two layers of plastic scintillators, each of

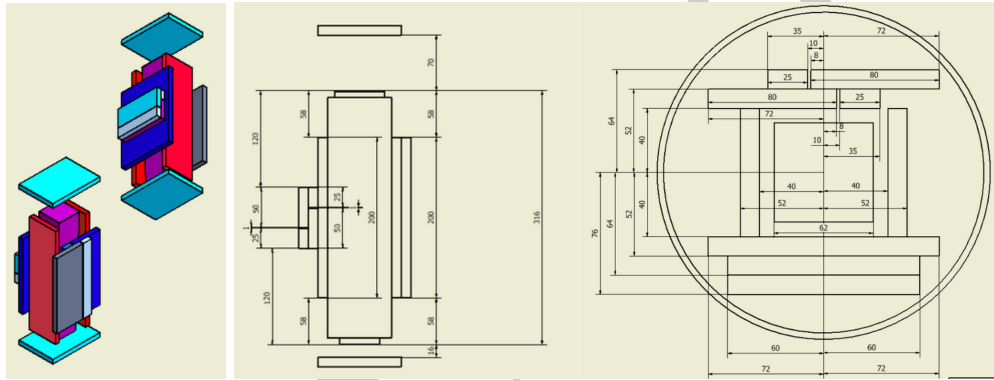


Figure 14: The CAD representation of the BDX-Hodo detector and some drawings with geometry and sizes.

them composed by a large and a small 1cm-thick scintillators strips. The overlap of the four paddles (each 20 cm long in Y) results in three independent 2.5 cm channels along the X (horizontal) direction. The same concept was applied to the back side of the crystal but with paddles tilted by 90 degrees to define three 2.5 cm independent channels along the Y (vertical) direction. The requirement of a hit in both front and back paddles defines a 3x3 matrix of $2.5 \times 2.5 \text{ cm}^2$ pixels providing a cm-like XY position resolution. The addition of a larger paddle ($20 \times 14.4 \text{ cm}^2$) on the back provides an enhanced sensitivity in the unlikely case rates will be much lower than what estimated by MC simulations. Four more paddles covering the left/right sides and the top/bottom of the crystal will be used to veto cosmic rays and other radiation not associated to the beam direction. The crystals will be coupled, on the large side, to a $6 \times 6 \text{ mm}^2$ Hamamatsu S13360-6025 SiPM as described in Sec. 3.2.1 of PR-16-001 [?]. The scintillator paddles will be made with extruded plastic, each read out via a WLS fiber coupled to a $3 \times 3 \text{ mm}^2$ Hamamatsu S12572-100 SiPM sharing the same technology used in the BDX Inner Veto detector (described in details in Sec. 3.2.2 of PR-16-001). Muons produced by the electron beam will be detected by requiring a 5-fold coincidence (two front paddles + CsI(Tl) crystal + two back paddles). The detector will be contained in a 20-cm diameter stainless-steel cylindrical vessel, covered on top and on the bottom by steel lids. The whole assembly will be water-tight to prevent any water leak inside the vessel. A stainless-steel extension to the top cover will be used to run signal and power cables from the detector to the ground. The extension,

made by a 1-inch stainless steel pipe, rigidly attached, will be used also to remotely control the cylinder rotation and provide a good accuracy in the define the angle wrt. the beam direction. The electronics necessary to record the 13 (scintillators) + 1 (crystal) channels require 1 fADC board inserted in a VME crate. The full DAQ system (crate + pc) will be host in a van parked close to the well entrance. The power will be provided by a diesel power generator to minimize the requirements of long extension cords.

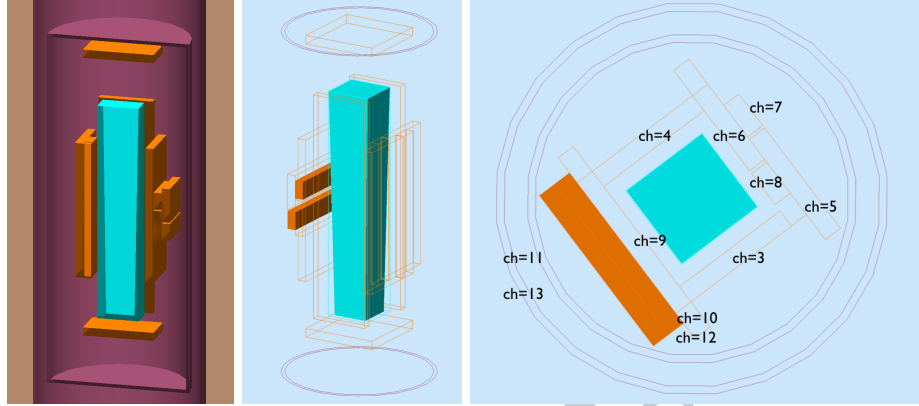


Figure 15: The GEMC implementation of the BDX-Hodo detector.

The detector geometry as well as the realistic response of the CsI(Tl) crystal and plastic scintillators have been implemented in GEMC (see Appendix B.2 of PR-16-001 [?] for details about the crystal and plastic scintillator response parametrisation). Figure ?? shows the BDX-Hodo implementation in GEMC. We assumed a detection threshold of 10 phe (in the scintillators and 100 phe in the crystal corresponding to 400 keV and 2 MeV of deposited energy respectively (MIPs release ~ 50 phe / 2 MeV and 1670 phe / 32 MeV respectively).

3 Results

Muons and beam-related background were produced by the 11 GeV electron beam interaction with the beam-dump and propagated in the region of interest as described in Sec. ??.

3.1 Muon detection

Fig. ?? shows the muon flux crossing the BDX-Hodo as obtained by GEMC and FLUKA in the three locations of interest (A, B and C). The flux has been sampled assuming the BDX-Hodo centred to the beam height. Results are reported for muons generated at high statistic by the custom μ event generator and propagated using GEMC (green points in the figure). The number of event generating at the dump correspond to $(1.2 \pm 0.1) 10^{12}$ EOT that correspond to a 0.2 uA

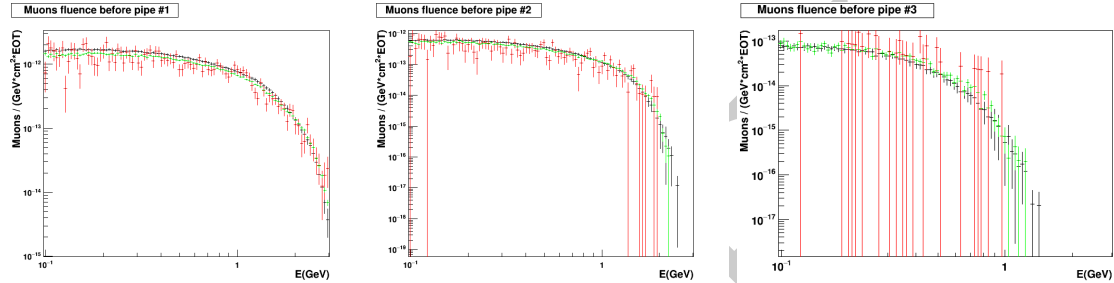


Figure 16: Muons energy spectra at the three locations of interest (A, B and C). Beam/dump interaction using FLUKA (black), GEMC (red) and the high statistic custom μ event generator with GEMC propagation (green).

3.2 Muon flux above the ground

For sake of completeness the muon flux has also been evaluated in the closest locations accessible above the beam-dump vault by using FLUKA. This set-up assumes to locate the detector above-the-ground with no drill required and simplifying the logistic of the tests. Due to the CPU-time necessary to track muons at such large angle (with respect to the beam axis) we used a two steps procedure. Firstly, the 11 GeV electron beam was let interact with the beam dump and muons produced on the roof of the vault has been sampled in three different position. Figure ??-left shows the four positions on the roof of the beam-dump vault where the flux has been sampled. A high statistic sample of muons have then been generated according to the previous distributions and propagated to the outside. Applying a conservative hypothesis (the muons are propagated perpendicular to the beam axis crossing the minimal amount of concrete and dirt) muons with energy higher than 4.5 GeV (the minimum to not been ranged out) were propagated and sampled in the three perpendicular locations outdoor. Figure ??-right shows the four locations (A_{Ext} , B_{Ext} , C_{Ext} , and D_{Ext}) on top of the hill. When integrated over the surface of the BDX-Hodo detector ($\sim 100 \text{ cm}^2$) and considering as a reference a beam current of $10 \mu\text{A}$, no sizeable muon flux would be detected ($\text{Rate}_{Max} < 3 \text{ Hz}$). Table ?? report the rates as obtained by the simulations.

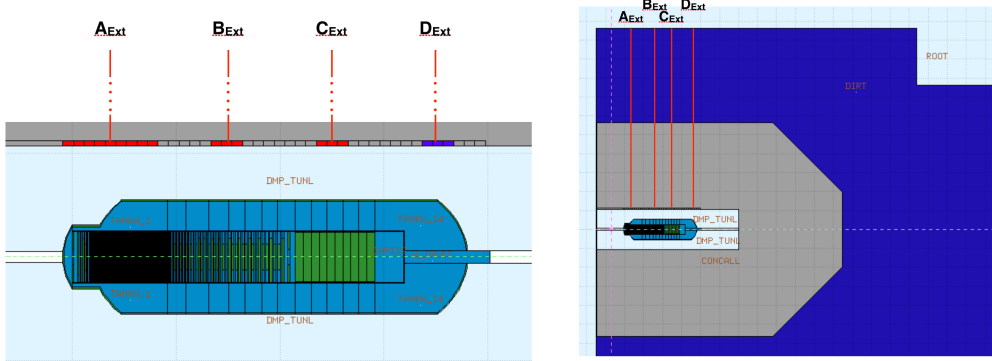


Figure 17: Left: In red are shown the points on the roof where muon flux has been sampled. Right: A_{Ext} , B_{Ext} , C_{Ext} , and D_{Ext} are the four location outdoor where the muon flux has been evaluated.

Table 1: Cosmic rate expected in different components of BDX-Hodo

Location	Rate _{Crystal} (Hz / (cm ² μA))
A_{Ext}	$2.2 \cdot 10^{-3}$
B_{Ext}	$4.7 \cdot 10^{-4}$
C_{Ext}	$1.9 \cdot 10^{-3}$
D_{Ext}	negligible

3.2.1 Beam-related background

Fig. ?? shows the neutron flux as obtained by FLUKA starting from the electron/beam-dump interaction in the three locations of interest.

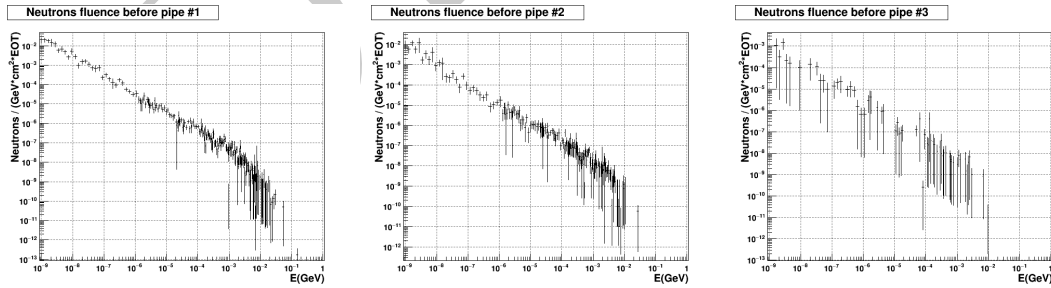


Figure 18: Neutron energy spectra at the three locations of interest. Spectra are obtained from electron beam interaction with the beam-dump using FLUKA.

3.2.2 Cosmic background

The cosmic muon background in the BDX-Hodo has been evaluated using GEMC. This is the same cosmic flux generator used in PR-16-001 [?]. The muon spectrum has been divided in different ranges and correctly weighted to estimate the full rate expected on the detector. Rates in the detector have been evaluated for CsI(Tl) crystal alone, Top scintillator alone (showing the maximum rate) and requiring the coincidence of the front/back scintillator with the crystal (the condition used to identify and count muons produced in the beam-dump). Detection thresholds were set to 10 phe and 100 phe for scintillators and CsI. Tab. ?? shows the results of this study. The cosmic rate is negligible (in every condition < 1 Hz) well below the expected rate of muons from the beam-dump.

Table 2: Cosmic rate expected in different components of BDX-Hodo

Energy range (GeV)	Rate _{Crystal} (Hz)	Rate _{Top Scintillator} (Hz)	Rate _{Coincidence} (Hz)
0.2 - 2	0.01	0.02	0
2 - 10	0.2	0.25	0.01
10 - 100	0.35	0.4	0.01
Cosmic muon rate	0.56	0.67	0.02

3.3 The test configuration

4 Appendix

4.1 Cost estimates

4.2 Work-plan, time-plan, ...

DRAFT